**Reviewer 1**

**Issue 1:**

The article describes a loose coupling scheme between fluid and solid for heat transfer calculations. The algorithm is validated with the solution of a reference problem and compared with other numerical results, and then it is used to solve and analyze the temperature distribution of a liquid rocket engine. The governing equations for the different modules involved in the simulation are given. The coupled strategy and the data transfer between non-matching meshes are presented, but the author does not validate the strategy and data transfer with a simple case.

**Discussion**

Thank you for your correction. We should use a simpler case to validate the algorithm. Due to the limitations of the article length, the results of the validation case presented below were not presented in the article.

The coupled heat transfer calculation is carried out for the hypersonic tube aerodynamic heating test. As shown in Figure 1, the experiment is conducted in an 8-foot high-temperature tunnel at NASA Langley [1]. The round tube with inner and outer diameter of 25.4mm and 38.1mm, respectively, is fixed in the wind tunnel with inlet Mach number of 6.47, regardless of the chemical non-equilibrium effect of inlet flow and given the initial cold wall temperature of 294.4K. The detailed free stream parameters and the material properties of the round tube are shown in Table 1 and Table 2. This experiment is a classic experiment to study the hypersonic aerodynamic heating of the front of a tube in the case of shock wave interference, and it is regarded by many researchers as a standard example of two-way fluid-structure coupling [2,3].

Table 1 Free stream parameters

| Parameter | Ma | Temperature (K) | Pressure (Pa) |
|---|---|---|---|
| Value | 6.47 | 241.5 | 648.1 |

Table 2 Material parameters

| Parameter | Density (kg/m$^3$) | Specific heat capacity (J/(kg • K)) | Conductivity (W/(m • K)) | Initial wall temperature (K) |
|---|---|---|---|---|
| Value | 8030 | 502.48 | 16.27 | 294.4 |

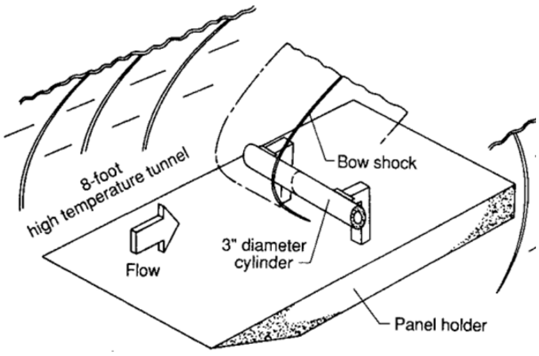


**Figure 1.** Experimental equipment

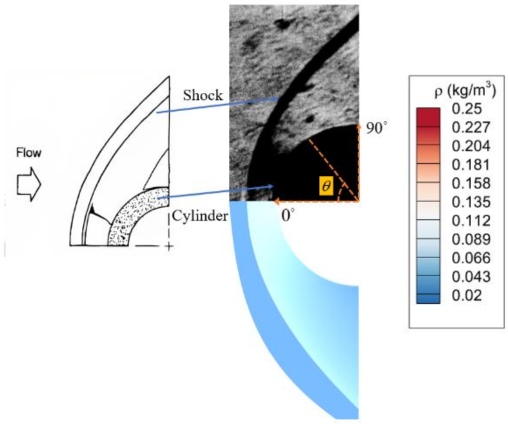


**Figure 2.** Experimental and numerical schlieren

Experimental schlieren and numerical schlieren are shown in Figure 2. The heat flux and pressure distribution on the outer wall of the round tube are respectively shown in Figure 3 and Figure 4. The $p_0$ and $q_0$ are the pressure and heat flux at the stagnation point, respectively. Both the temperature and pressure at the stagnation point reach the maximum value, which is in good agreement with the experimental data in the literature. Based on the initial flow field, unsteady coupled heat transfer is calculated in this paper, and the heat transfer time step is 0.1s.

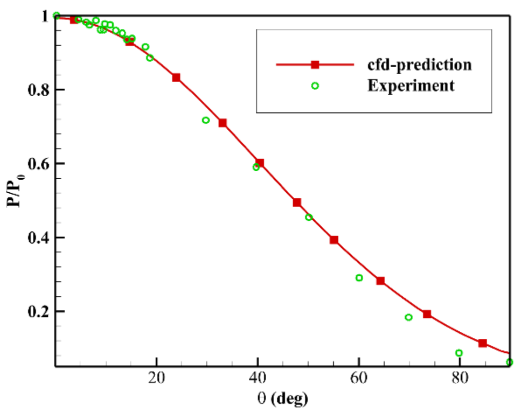


**Figure 3.** Wall pressure distribution

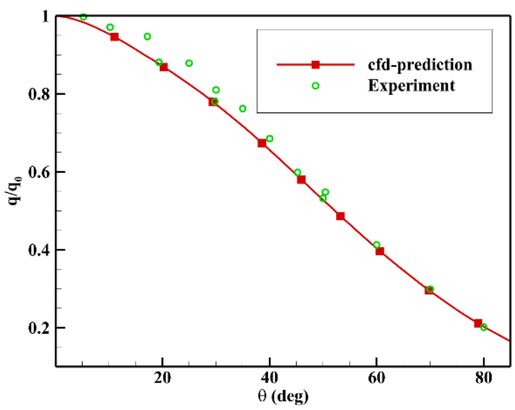


**Figure 4.** Wall heat flux distribution

Figure 5 shows the change of temperature at the stagnation point of the leading edge of the tube over time, which is similar to the calculation results of other researchers. The calculated stagnation temperature at 5s is 470.03K, and the experimental measurement is 476.67K, with an error of only 1.39%. The temperature distribution on the outer surface of the tube in the fifth second (as shown in Figure 6) has a certain deviation from the measured value in the experiment. However, the experiment obtains hypersonic airflow by burning methane and air in a high-pressure combustion chamber, so the gas component contains methane combustion products, which is different from the flow parameters given here.

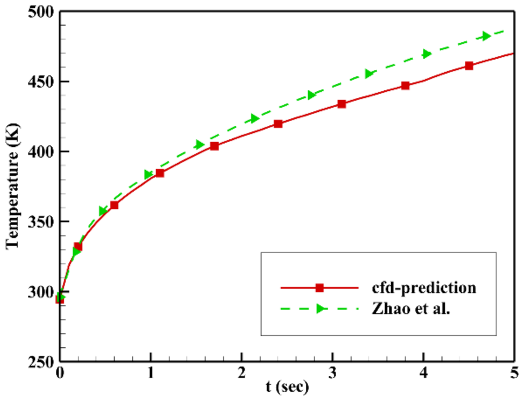


**Figure 5.** Variation of stagnation temperature with time

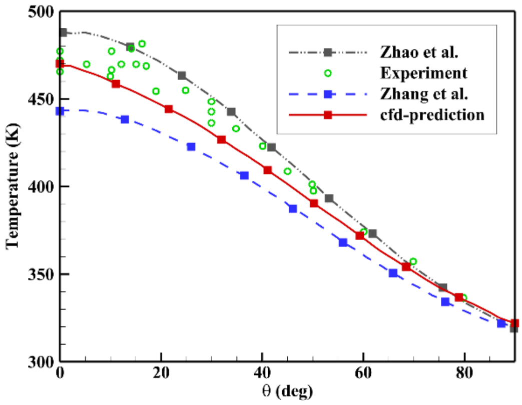


**Figure 6.** Temperature distribution of tube surface at 5th second


1. Wieting A R, Holden M S. Experimental shock-wave interference heating on a cylinder at Mach 6 and 8, AIAA Journal, 1989, 27(11): 1557-1565.
2. Zhang S, Chen F, Liu H. Time-adaptive, loosely coupled strategy for conjugate heat transfer problems in hypersonic flows, Journal of Thermophysics and Heat Transfer, 2014, 28(4): 635-646.
3. Zhao X, Sun Z, Tang L, et al. Coupled flow-thermal-structural analysis of hypersonic aerodynamically heated cylindrical leading edge, Engineering Applications of Computational Fluid Mechanics, 2011, 5(2): 170-179.


**Issue 2:**

They simulate a high-enthalpy nozzle and compare the wall temperature at the throat, which roughly matches the numerical reference results. After that, they solved a more complex liquid engine nozzle, obtaining the wall temperature and fluxes. Also, they simulated the effect of the film cooling, but no details are given about how it was introduced in the simulation process.

**Discussion**

Thank you for your correction. We have added the treatment method for film cooling in the article. We added the gas film to the source term of the N-S equation.

$$\frac{\partial \boldsymbol{U}}{\partial t}+\nabla\cdot[\boldsymbol{F}(\boldsymbol{U})-\boldsymbol{G}(\boldsymbol{U})]=\boldsymbol{S}$$

This engine has a large size and a high combustion chamber temperature, resulting in a very short liquid film length. Therefore, we simplify the process of spray atomization and liquid film cooling, treating all propellants entering the combustion chamber as gas. At the location of the gas film injection point in the flow field, we added the gas film to the source term of equation (1) based on the mass flow rate, velocity, and other parameters of the gas film.

**Issue 3:**

It is not clear what the original contribution of the article is. What are the benefits of this algorithm when compared with others in the literature?

**Discussion**

Thank you for your question. The main original contribution and scientific novelty of this article is to provide a feasible method for calculating the heat transfer of liquid rocket engines including film cooling, regenerative cooling, radiation cooling, and other cooling methods, providing a scalable and efficient framework for related software. As a loosely coupled method, convergence and stability are its advantages. The corresponding content of this article has been modified as follows:

In the literature we have reviewed, there is relatively little research on the coupled heat transfer mechanism of multiple physical regions in liquid rocket engines. The mechanism of data transfer between different computing regions, the solution flow chart of the coupled heat transfer problem, convergence criteria, and so on are lacking.

In this paper, a platform with strong extensibility and high stability for heat transfer calculation of composite cooling liquid rocket engines was provided, and a corresponding numerical method was presented.

**Issue 4:**

Comments about the title: The word "fluid-structure" is used in the title, but only solid heat conduction is solved, not structural deformation/interaction, so I recommend rewriting it to be more explicit about the scope of the paper.

**Discussion**

Thanks for your advice. Following your advice, we have corrected the title of the paper. The new title is “A coupled heat transfer calculation strategy for composite cooling liquid rocket engine”. It only emphasizes the heat transfer process between fluid and structure.

**Issue 5:**

L13: the method of parameter transfer -> the data is transferred between meshes, not the parameters.

**Discussion**

Thank you for your correction. We have checked and rewritten this part.

The numerical method used in each physical area, the method of data transfer between each computing module, the strategy of data transfer on the coupling interface, the calculation process, and the convergence criterion were introduced in detail.

**Issue 6:**

L20: What is the meaning of "relatively reasonable"?

**Discussion**

Thank you for pointing out the error in our expression. The calculation results in this article are reasonable. The numerical results of the AEDC high enthalpy nozzle are in good agreement with experimental measurement and other researchers. The distribution trend of wall temperature and heat flux in the calculation results of rocket engines is correct. Therefore, we delete the word 'relatively'.

The results showed that the algorithm successfully indicated the protective effect of the gas film on the wall surface, and the calculation results were reasonable.

**Issue 7:**

L41: ...which is a typical fluid-structure coupled heat transfer problem. It is a fluid-solid heat transfer problem.

**Discussion**

Thank you for your correction. We have modified this part.

Heat transfer in the thrust chamber involves many physical processes, including the combustion and flow in the thrust chamber, the convection and radiation heat transfer of high-temperature gas to the wall, heat conduction inside the wall, heat transfer between the coolant and wall in the cooling channels, and radiation heat transfer between the outer wall and the surrounding environment and so on, which is a typical fluid-structure heat transfer problem.

**Issue 8:**

L110: No mention is made about the algorithm or discretization for the gas flow in the chamber.

**Discussion**

Thanks for your advice. We have added the introduction of the algorithm and discretization for the gas flow in the chamber.

The three-dimensional Navier-Stokes (N-S) equation is discretized by the density-based finite volume method to solve gas flow. The chemical equilibrium laminar flamelet model was used to calculate the turbulent combustion in the thrust chamber.

**Issue 9:**

L155: Euken and lennard-jone formulas should be added.

**Discussion**

Thanks for your advice. We have added Eucken’s formula, Lennard-Jone’s formula and relevant references in the paper.

Where $\mu$ is the viscosity coefficient, Pr is the Prandtl number, Sc is the Schmidt number and the subscript $t$ denotes turbulence. Turbulent parameters are determined by the SST $k-\omega$ model. Among the properties used in this paper, the thermal conductivity $\kappa_i$ and dynamic viscosity coefficient $\mu_i$ are determined by Eucken's formula [35] and Lennard-Jone's formula [36], respectively. The properties of mixtures, such as viscosity coefficient $\mu$, diffusion coefficient $D$, and heat conduction coefficient $\kappa$, are calculated by Wilke's mixing rules. Eucken's formula and Lennard-Jone's formula are presented in Appendix A.

**Appendix A**

Eucken's formula:

$$\kappa_i = \frac{\mu_i R_0}{W_i}\left(c_{pi}\frac{W_i}{R_0}+\frac{5}{4}\right)$$

Where $\kappa_i$ is the thermal conductivity coefficient, $\mu_i$ is the dynamic viscosity coefficient, $W_i$ is the molar mass, $R_0$ is the universal gas constant, $c_{pi}$ is the specific heat at constant pressure.

Lennard-Jone's formula:

$$\mu_i = 2.6693\times 10^{-6}\frac{\sqrt{W_i T}}{\sigma_i^2 \Omega_{\mu_i}}$$

Where $\mu_i$ is the dynamic viscosity coefficient, $W_i$ is the molar mass, $T$ is the static temperature, $\sigma_i$ is the Lennard-Jones collision diameter and its unit is Angstroms. $\Omega_{\mu_i}$ is the collision integral and its expression is:

$$\Omega_{\mu_i} = 1.147\left(T^*\right)^{-0.145} + \left(T^* + 0.5\right)^{-2}$$

Where $T^*$ is the reduce temperature and its expression is:

$$T^* = \frac{k_B T}{\varepsilon_i}$$

Where $k_B$ is the Boltzmann constant, $\varepsilon_i$ is the Lennard-Jones well depth.

35. Anderson J. D. Hypersonic and High-Temperature Gas Dynamics, Second Edition. New York: McGraw-Hill,2006: 696-699.

36. Reid R. C., Prausnitz J. M., Sherwood T.K. The Properties of Gases and Liquids, Third Edition, New York: McGraw-Hill, 1977.

**Issue 10:**

L166 to 175: Undefined acronyms are used without their definitions.

**Discussion**

Thank you for your correction. We have defined these acronyms in the paper. Now, the ‘N-S equation’ and the ‘UDMH/NTO’ has been defined in the introduction. The ‘HLLC’ comes from the abbreviation of the research's name and does not require further explanation.

In this paper, the finite volume method is used to discrete the N-S equation. The HLLC scheme is used for the spatial discretization of the circulating flux. The standard center scheme is used for the discretization of viscous flux. The implicit Lower-upper symmetric Gauss-Seidel (LU-SGS) scheme is used to solve equations. The UDMH/NTO two-parameter indexed instantaneous laminar flamelet table $Y_i(z,z''^2)$ is generated by the Fluent software. The concentration of each component in the flow field is obtained by the flamelet table. Temperature is obtained by solving the energy equation, not the flamelet table. In other words, the flamelet table is used as a complex equation of state to describe the relationship between local temperature and composition, density, pressure, etc.

**Issue 11:**

L177: Structural heat conduction -> Solid heat conduction

**Discussion**

Thank you for your correction. We have modified it in the paper.

**Issue 12:**

L225: Parameter transfer policy -> Data transfer scheme

**Discussion**

Thank you for your correction. We have modified it in the paper.

**Issue 13:**

L226 to 228: The paragraph should be rewritten.

**Discussion**

Thank you for your suggestion. We have rewritten this paragraph.

Figure 1 shows the data transfer between different computing regions. The principle of data exchange is to ensure that the temperature and heat flux of the fluid and solid at the coupling interface remain continuous. It can be expressed as:

$$T_{solid} = T_{fluid}, q_{solid} = q_{fluid}$$

**Issue 14:**

L245: Parameter transfer policy between codes. -> Data transfer between codes.

**Discussion**

Thank you for your correction. We have modified it in the paper. We have checked the article and corrected all similar incorrect expressions.

**Issue 15:**

L237 to 240: The paragraph is difficult to understand. Rewrite.

**Discussion**

Thank you for your correction. We have rewritten this paragraph.

For solid and fluid regions, the boundary conditions used at the coupling interface are different. The temperature boundary condition is used in the fluid regions such as the flow field in the thrust chamber and the regenerative cooling channel, and the heat flux boundary condition is used in the solid regions. The convective heat flux on both sides of the wall is calculated by the fluid solvers. Then the gas radiation module will read the temperature, pressure, and mass fraction of the $CO_2$ and $H_2O$ in the flow field and output the radiant heat flux. Then, the heat flux on both sides of the wall will be input into the heat conduction module to calculate the temperature on both sides of the wall.

The above steps will be repeated until the calculation converges. To improve the stability of the calculation, the temperature and heat flux data transferred at the coupling interface are under-relaxed.

**Issue 16:**

Caption Fig. 1 - Rewrite: Data transfer between codes.

**Discussion**

Thank you for your correction. We have rewritten this figure caption.

**Issue 17:**

L250: Number of grids? Do you mean element size?

**Discussion**

Thank you for pointing out the inadequacies in our expression. Linear interpolation is not an interpolation method that can guarantee the conservation of flux. To reduce the impact of inaccurate interpolation on the calculation results, the grid should be relatively dense, in other words, the grid element size should be small. We have corrected this sentence in the paper.

This method is simple to operate, has a clear physical meaning, and can achieve high precision when the grid is dense.

**Issue 18:**

L291: AEDC should be defined when it is first used.

**Discussion**

Thank you for your correction. We have defined these acronyms before using it.

The feasibility and efficiency of the coupled heat transfer strategy are checked by two representative cases The first case is the Arnold Engineering Development Center (AEDC) high enthalpy nozzle flow, and the second case is a liquid rocket engine.

**Issue 19:**

No information about the numerical setup, grid sizes, or initial conditions are given. Is the problem solved in 2D, axisymmetric or 3D?

**Discussion**

Thank you for your correction. We have added these contents to the paper.

Figure 5 shows the grid of the nozzle. The quantity of the cells is 71282. The area with a circumferential direction of 2° of the chamber is selected as the computational domain. The calculation parameters are shown in Table 2.

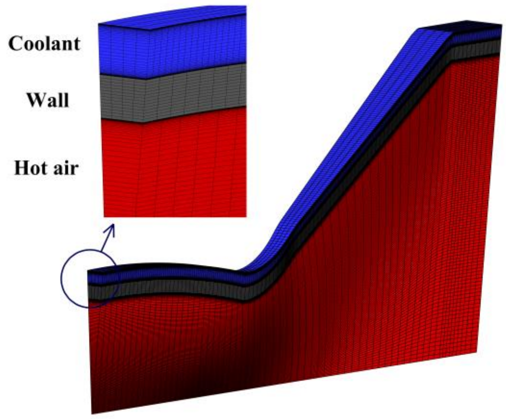


**Figure 5.** The grid of the AEDC nozzle.

**Table 2.** Calculation parameters of the AEDC nozzle

| **Air total pressure (atm)** | **Air total temperature (K)** | **Water mass flow rate (kg/s)** | **Water inlet temperature (K)** |
|---|---|---|---|
| 126.5 | 5000 | 5.234 | 309 |

**Issue 20:**

Fig.4 What is the meaning of a segmented and continuous nozzle?

**Discussion**

Thank you for your correction. As shown in the following figure, this is the segmentation made by Shope in the schematic diagram of the AEDC nozzle, which means two cooling channels, each with its inlet and outlet. To avoid misunderstandings, we have renamed it 'Segent 1' and 'Segent 2'.

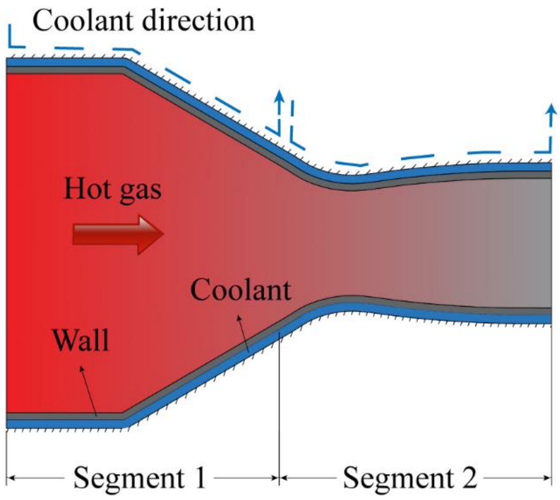


**Figure 4.** The configuration of the AEDC nozzle.

**Issue 21:**

L324: No reference to the experimental data is given.

**Discussion**

Thank you for your correction. We have added the reference which contains experimental data.

The temperature rise of water in the calculation result is 12.7K, which is slightly lower than the temperature rise measured in the test of 13.9K [42]

42. Shope F L. Conjugate conduction-convection heat transfer with a high-speed boundary layer, Journal of thermophysics and heat transfer, 1994, 8(2): 275-281.

**Issue 22:**

L352: Any detail about the meshes(solid, fluid, etc) used in the simulations is given.

**Discussion**

Thank you for your suggestion. We have added the grid information to the paper.

Figure 8(a) and Figure 8(b) show the grids of typical spiral and straight cooling channels, respectively. The blue area in the figure represents the fluid grid, while the gray area represents the solid grid. Only the 2° area in the circumferential direction of the thrust chamber was taken for the calculation. The flow field grid in the thrust chamber is shown in Figure 9(a). Periodic boundary conditions were used on both sides of the area in the circumferential direction. Three sets of grids were used to verify the grid independence of the flow field in the thrust chamber, with the number of grids increasing in sequence. Figure 9(b) shows the heat flux along the wall computed by using the three different grids. Mesh 3 was adopted in this study.

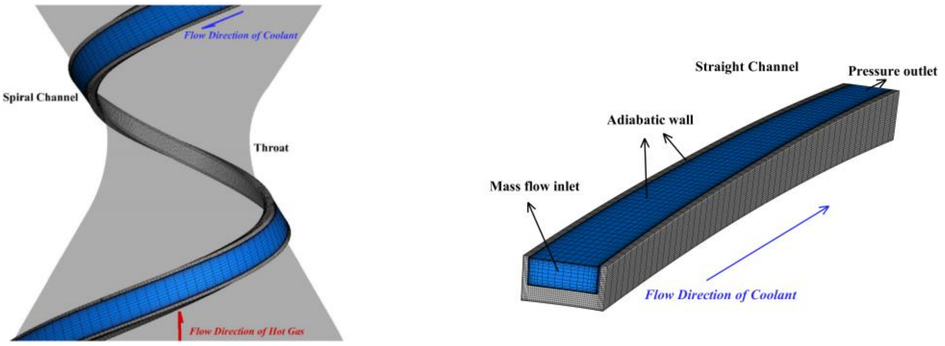


(a) (b)

**Figure 8.** (**a**) Grid of spiral cooling channel at the throat; (**b**) Grid of straight cooling channel at the expansion section.

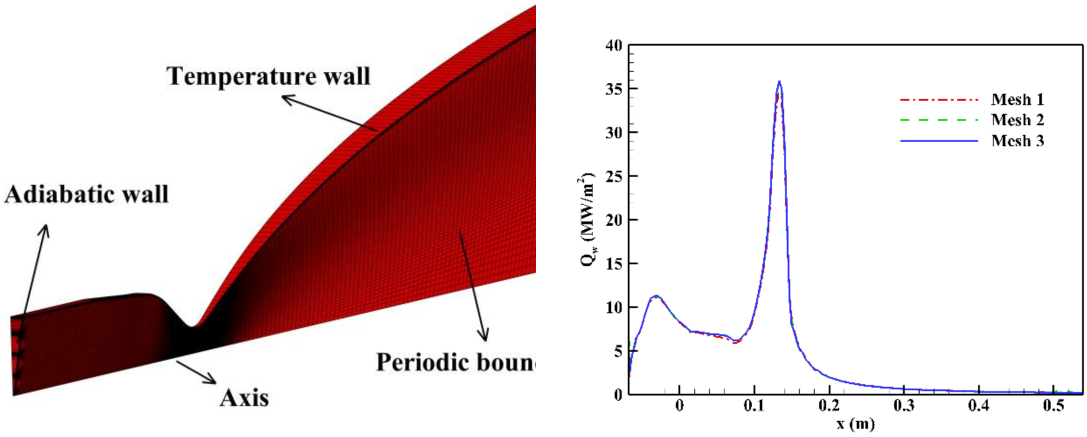


(a) (b)

**Figure 9.** (**a**) The grid of flow field in the chamber; (**b**) Heat flux along the wall.

**Issue 23:**

L439: Only the experimental coolant temperature rise is given.

**Discussion**

Thank you for your correction. We have rewritten this sentence.

The coolant temperature rise in the numerical simulation results is in good agreement with experimental measurement, which proves the effectiveness of the algorithm.

**Issue 24:**

English should be checked carefully.

**Discussion**

Thank you for your suggestion. We have checked the English expression of this article and corrected some syntax errors.